

Short Communication

Influence of AC Interference on the Corrosion Behavior of 2507 Super Duplex Stainless in Simulated Concrete Pore Solution

Min Zhu^{1,*}, Baozhu Zhao¹, Li Liu², Yongfeng Yuan¹, Shaoyi Guo¹

¹ School of Mechanical Engineering & Automation, Zhejiang Sci-Tech University, Hangzhou 310018, China,

² Interplex Electronic (HZ) Co., Ltd, Hangzhou 310018, China

*E-mail: zmii666@126.com

Received: 27 July 2020 / Accepted: 11 September 2020 / Published: 30 September 2020

The corrosion behavior of 2507 super duplex stainless steel (SDSS) interfered by AC in simulated concrete pore solution containing Cl^- was studied in this work. The results show that a rapid increase in i_p and an apparent drop in E_p as well the significant decrease in R_f and R_{ct} values suggest that the addition of Cl^- and applied AC result in an obviously harmful effect on the passive film, and enhance the dissolution rate of film. The change in N_D and N_A values indicates that the presence of Cl^- or AC application reduce the compactness of film, increase the amount of defects, and weaken the protective ability. Especially at the combined action of Cl^- and imposed AC, the instability of passive film becomes much worse, causing a further decrease in the anti-corrosion resistance of SDSS. AC facilitates the adsorption of Cl^- and H^+ ions on the defects within passive film.

Keywords: Corrosion behavior; Imposed AC; Protective ability; Passive film

1. INTRODUCTION

Up to now, increasing stainless steels served as the rebar have been widely employed in the concrete structure, because of the excellent comprehensive properties of strong corrosion resistance, high mechanical performances and long service time [1,2]. Some research works have reported the corrosion behavior of stainless steels in simulated concrete environments [3-5]. Alonso [6] indicated that the anti-corrosion property of DSS in a solution with Cl^- ions could be affected by the Ni content. Moser [7] found that UNS S32304 and S32205 exhibited a good anti-stress corrosion cracking ability when Cl^- concentration was below 0.5M. At present, 2507 SDSS has been widely employed in many engineering structures because of excellent anti-corrosion resistance [8,9]. Nevertheless, the literature regarding the corrosion behavior of 2507 SDSS used in the simulated concrete pore solution is rare.

AC interference is frequently detected in the seashore regions close to super-high voltage transmission lines [10,11]. When 2507 SDSS used as rebar in concrete structure is closed to AC electric field, the surface passive film with outstanding corrosion resistance may be damaged, accelerating the corrosion failure of SDSS rebar concrete structure used in this region. However, there is no report on the influence of Cl^- and AC on corrosion behavior of 2507 SDSS in simulated concrete environment. Hence, the AC corrosion behavior of 2507 SDSS served as rebar material in simulated concrete pore solution containing Cl^- was investigated in this paper.

2. EXPERIMENTAL

2.1. Material and solution

The chemical composition (wt.%) of SAF2507 SDSS is as below: C 0.018, Si 0.47, Mn 0.75, P 0.023, S 0.001, Cr 25, Ni 6.92, Mo 3.89, N 0.269 and Fe balance. The specimen with dimension of 10 mm×10 mm×5 mm was sealed with epoxy resin, leaving an exposed region of 1 cm². Then, the sample was successively polished, washed and air dried. The saturated $\text{Ca}(\text{OH})_2$ solution with a pH value of about 12.6 as the simulated concrete pore solution was used to conduct the related tests [12,13]. To study the influence of Cl^- on corrosion behavior of potential rebar-2507 SDSS, 3.5% Cl^- was added to the saturated $\text{Ca}(\text{OH})_2$ solution.

2.2. Electrochemical tests

All tests were conducted at three conditions. With or without the addition of Cl^- ions, the electrochemical tests were conducted via PARSTAT2273 electrochemical workstation with a three-electrode cell. The specimen was served as the working electrode, a large area pt sheet as a counter electrode, and a saturated calomel electrode (SCE) as a reference electrode. Open circuit potential (OCP) curve of SDSS was tested for 0.5h. The potentiodynamic polarization curve was tested with a scan rate of 0.5mV/s from -1.2 V (vs. SCE) to 1.2 V (vs.SCE). To study the effect of imposed AC on the corrosion behavior, the SDSS electrode was applied with AC of 100A/m² in saturated $\text{Ca}(\text{OH})_2$ solution containing 3.5% Cl^- during the whole testing process. The sketch diagram of AC corrosion is identical to that in our previous researches [14,15]. A 50 Hz sine AC was imposed to the SDSS sample.

To inquiry the influence of Cl^- and AC on passive film formed on the electrode surface, the electrochemical impedance spectroscopy (EIS) and Mott–Schottky curve were tested. With or without the presence of Cl^- to the saturated $\text{Ca}(\text{OH})_2$ solution, the passive films were grown at a constant potential of 0.42V for 1h via the potentiostatic polarization. For the third testing condition, AC was imposed to the film formed in the solution with 3.5% Cl^- for 5 min. Subsequently, the two measurement methods were used to assess the effect of different testing conditions on the film. EIS curve was performed at OCP within the frequency range of 100 kHz to 10 mHz with a interference

signal amplitude of 10 mV. Then, Mott–Schottky curve was conducted at 1 kHz from -1.0 V to 1.0 V with 50mV/step. The above tests were conducted at 25°C.

3. RESULTS

3.1 Open circuit potential

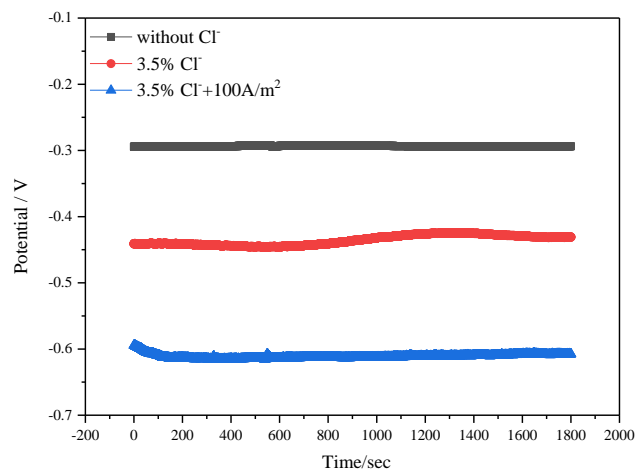


Figure 1. Open circuit potential curves of SDSS without or with Cl^- and AC interference

Figure 1 shows the open circuit potential curves of SDSS tested at different conditions. When no Cl^- ions are added into the saturated $\text{Ca}(\text{OH})_2$ solution, the OCP value of SDSS is the nobler. After adding 3.5% NaCl to the solution, the curve shifts downward, that is, the OCP value reduces. This indicates that the addition of Cl^- increases the corrosion trend of SDSS. When i_{AC} of $100\text{A}/\text{m}^2$ is applied, a further decrease in the OCP value is revealed. This suggested that the presence of Cl^- and the application of AC generate a combined effect, promoting the electrochemical activity.

3.2 Polarization curve

Figure 2 displays the polarization curves of SDSS measured at different conditions. A significant difference in the anodic branch is observed. The shape of curve without Cl^- is similar to that of with Cl^- . However, after the addition of Cl^- to the saturated $\text{Ca}(\text{OH})_2$ solution, the curve shift rightward. In the presence of AC, the passive region becomes narrow, with a low pitting potential (E_p). The fitted passive current density and pitting potential of SDSS are shown in Figure 3. At the condition of without Cl^- , the SDSS has the lowest i_p and the highest E_p value. SDSS in the saturated $\text{Ca}(\text{OH})_2$ solution containing 3.5% Cl^- has lower E_p and larger i_p value than those of without Cl^- . This means that the corrosion resistance of SDSS is declined due to the existence of Cl^- . In the case of imposed AC, a rapid increase in i_p as well an apparent drop in E_p suggest that applied AC and the addition of Cl^- create a combine effect, reducing the passivity and anti-corrosion property of SDSS.

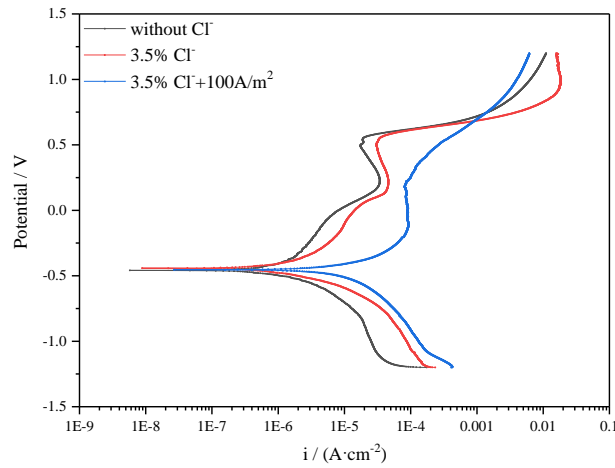


Figure 2. Polarization curves of SDSS without or with Cl⁻ and AC interference

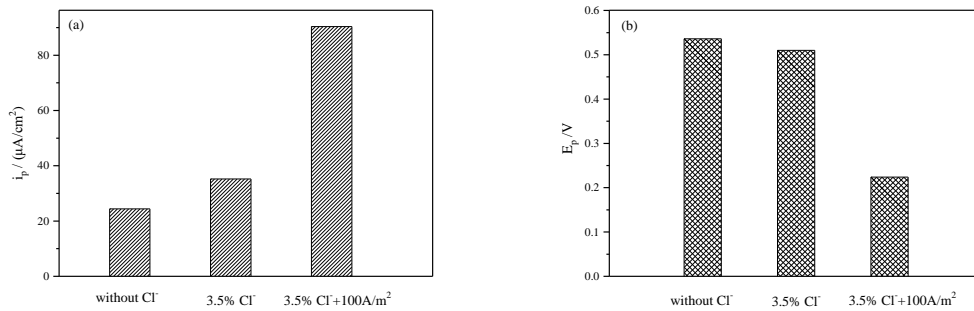
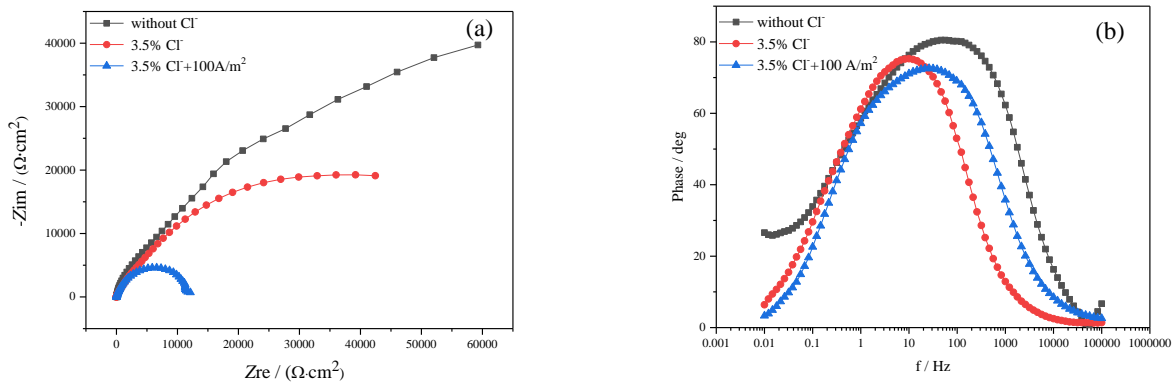


Figure 3. Passive current density and pitting potential of SDSS without or with Cl⁻ and AC interference (a) i_p ; (b) E_p

To further analyze the effect of Cl⁻ and AC on the passivity of SDSS, EIS and Mott-Schottky curve were adopted to study the theme.

3.3 EIS test



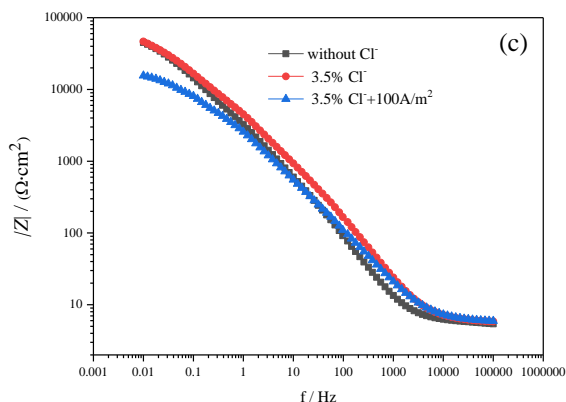


Figure 4. Impedance spectra of SDSS without or with Cl^- and AC interference (a) Nyquist plot; (b and c) Bode plots

Figure 4 exhibits the impedance spectra of SDSS tested at different conditions. The three curves in Fig.4a exhibit the apparent characteristics of capacitive reactance. In the absence of Cl^- , the SDSS sample has the maximum arc radius. After adding Cl^- to the saturated $\text{Ca}(\text{OH})_2$ solution, the arc radius declines. Whereas the presence of AC further decreases the arc radius. Meanwhile, the SDSS sample without Cl^- possesses the maximum phase angle in medium frequency region, followed by that of with Cl^- , and the angle is the lowest at the condition of 3.5% $\text{Cl}^- + 100\text{A}/\text{m}^2$.

In addition, the impedance value at 10 mHz is the minimum under the combine action of Cl^- and AC. These features imply that the passive film formed on the surface of SDSS without Cl^- exhibits the excellent corrosion resistance [16].

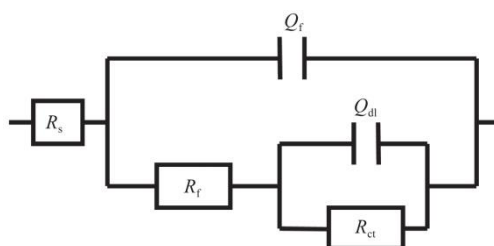


Figure 5. Equivalent circuit for fitting EIS data.

Using the equivalent circuit (Figure 5) to fitting the impedance spectra, the results are listed in Table.1. R_s is the solution resistance, Q_f represents the capacitance of passive film, R_f denotes the resistance of passive film. Q_{dl} is double-layer capacitance and R_{ct} corresponds to the charge transfer resistance. As shown in Table.1, the SDSS specimen without Cl^- has the largest values of R_f and R_{ct} , which indicates that the compact and complete passive film exhibits the optimal protective property. R_{ct} represents the difficulty degree of charge reaching the interface of electrode substrate through its

surface passive film. The presence of Cl^- drops the R_f and R_{ct} values, which implies that the addition of Cl^- destroys the completeness of the film, weakening the protective ability. When AC is applied, the significant decrease in the two index value suggests that the charge and species easily penetrate the damaged film due to the decreased resistance. Hence, the anti-corrosion resistance of SDSS is markedly decreased under the condition of 3.5% $\text{Cl}^- + 100 \text{ A/m}^2$.

Table 1. Electrochemical parameters of SDSS tested at different conditions

Conditions	$R_s/$ $\Omega \cdot \text{cm}^2$	$Q_f/$ $10^{-5} \text{F} \cdot \text{cm}^2$	$R_f/$ $\Omega \cdot \text{cm}^2$	$Q_{d1}/$ $10^{-5} \text{F} \cdot \text{cm}^2$	$R_{ct}/$ $10^4 \Omega \cdot \text{m}^2$
A	5.77	5.353	6245	7.184	8.35
B	5.617	5.663	1690	7.671	7.086
C	5.654	6.163	345	8.008	1.173

Noted: A: without Cl^- ; B: with 3.5% Cl^- ; C: with 3.5% $\text{Cl}^- + 100 \text{ A/m}^2$

3.4 Mott-Schottky curve

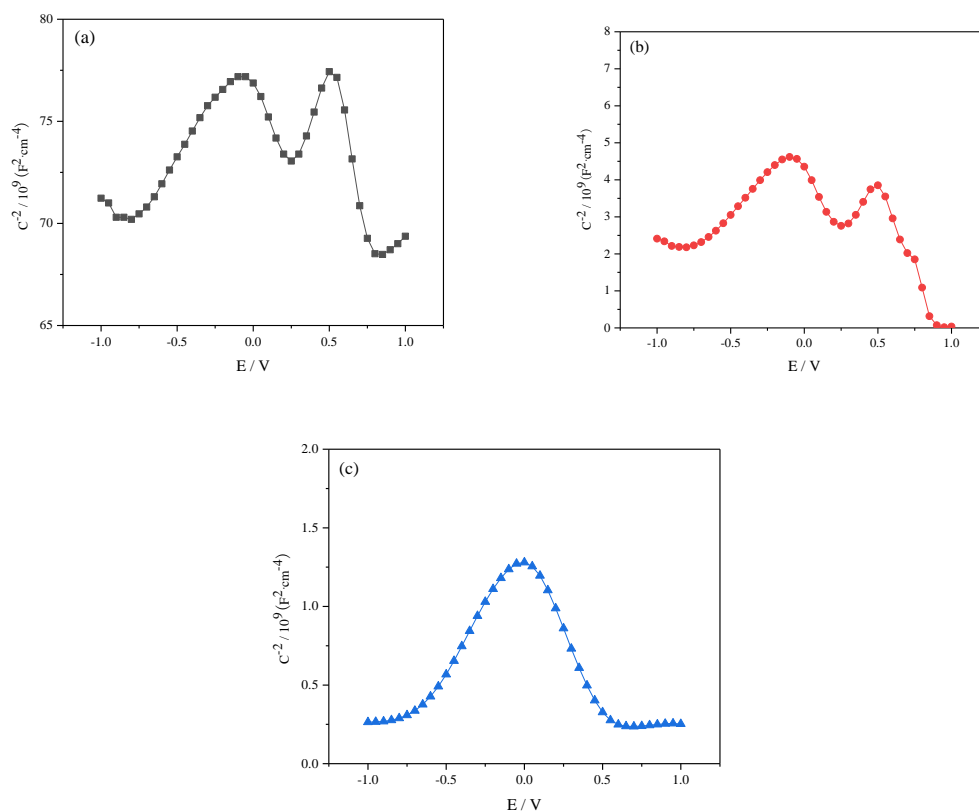


Figure 6. Mott-Schottky curves of SDSS tested at different conditions (a) without Cl^- , (b) 3.5% Cl^- , (c) 3.5% $\text{Cl}^- + 100 \text{ A/m}^2$

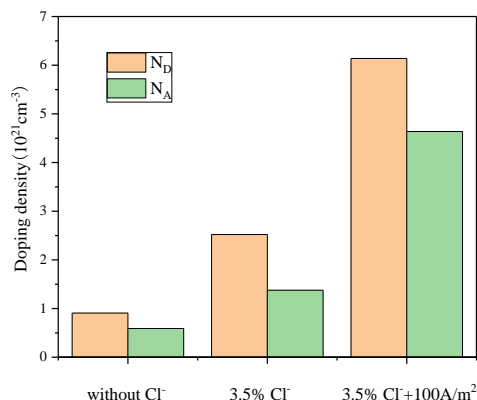


Figure 7. N_D and N_A values of passive films of SDSS without or with Cl^- and AC interference

The change in the structure of passive film was studied by Mott-Schottky curve. The correlation between space charge capacitance (C) and applied potential can be described by the Mott-Schottky equations (1) and (2):

$$\frac{1}{C^2} = \frac{2}{\varepsilon \varepsilon_0 e N_D} \left(E - E_{fb} - \frac{kT}{e} \right) \quad \text{for n-type semiconductors} \quad (1)$$

$$\frac{1}{C^2} = -\frac{2}{\varepsilon \varepsilon_0 e N_A} \left(E - E_{fb} - \frac{kT}{e} \right) \quad \text{for p-type semiconductors} \quad (2)$$

where e is the electron charge ($1.602189 \times 10^{-19} \text{ C}$), ε denotes the relative dielectric constant of the passive film, ε_0 is the permittivity of the vacuum ($8.854 \times 10^{-12} \text{ F}\cdot\text{m}^{-1}$), T is the Kelvin temperature, k is Boltzmann's constant ($1.38 \times 10^{-23} \text{ J}\cdot\text{K}^{-1}$), E is the applied electrode potential (V vs. SCE), and E_{fb} represents the flat band potential (V vs. SCE). N_D and N_A are the donor and acceptor densities (cm^{-3}) of n-type and p-type semiconductors, respectively, which can be gained from the positive and negative slopes of the linear portions in Mott-Schottky curve.

In Figure 6, there is a marked difference in the shape of curves. Among them, the shape of curve with 3.5% Cl^- is analogous to that without Cl^- , whereas the combined action of Cl^- and AC significantly changes the shape of curve. In the potential range of -1.0 V to 1.0 V, the first two curves have two peaks, with the semiconductor characteristics of n-p-n-p. In the presence of imposed AC, the curve measured in the solution containing 3.5% Cl^- exhibits only one peak, with the semiconductor feature of n-p type. As revealed in Figure 7, the passive film without Cl^- has lower N_D and N_A values compared with that in the solution containing Cl^- . Under the combined action of Cl^- and AC, the two index values remarkably increase. This implies that the addition of Cl^- or application of AC enhance the amount of defects within the film. The broken film is conducive to supplying more channels for the charge transfer, hence, the electrode reaction can be facilitated. Therefore, the change in N_D and N_A values suggests that the presence of Cl^- or AC application reduce the compactness of film, increase the amount of defects, and decline the corrosion resistance. Especially at the condition of Cl^- and AC, an obviously harmful effect on the passive film is exhibited.

After adding 3.5% Cl^- to the saturated $\text{Ca}(\text{OH})_2$ solution, a great amount of Cl^- ions can absorb on the surface of passive film. Generally, the presence of aggressive ion Cl^- would react with oxygen vacancy, and form the cationic vacancy[17]. The passive film may be damaged due to the cationic

vacancy concentrated at the interface of film/substrate. The increase in N_D and N_A values imply that the presence of Cl^- results in the information of passive film with disordered structure[18,19], promoting the pitting sensitivity. When AC is applied, the diffusion rate of charge ions (e.g., Cl^- , H^+ , Fe^{2+}) in the electrolyte solution can be enhanced, hence, more number of Cl^- ions can absorb on the film. That is, the applied AC is more harmful to the passive film.

Furthermore, the variation of film thickness on the surface of SDSS tested at different conditions can also evaluate the difference in anti-corrosion resistance, which can be calculated by the below equation [20]:

$$d = \left[\frac{2\varepsilon\varepsilon_0(E - E_{fb} - \frac{\kappa T}{e}) / e}{eN_D} \right]^{1/2} \quad (3)$$

The parameter values in this equation are the same as above. According to the equation, the increase of N_D value means that the existence of Cl^- or AC interference can thin the thickness of passive film, especially at the combined influence of Cl^- and imposed AC. Therefore, the protective capability of film would be weakened.

Similarly, when AC is applied, more H^+ ions can absorb on the film surface because the fast migration rate[21]. In addition, in the negative half-cycle of AC, the accumulation of negative charge can attract a large amount of H^+ , and absorb on the film surface. These H^+ ions react with O_2 , causing the generation of anionic oxygen vacancies[22]. These defects affect the occurrence of redox reaction, and enhance the dissolution rate of film.

Our previous research [14] found that the applied AC facilitated the hydrogen evolution reaction and generated massive H protons. These protons concentrate at some active micro-areas, resulting in the adsorption of Cl^- ions[23,24]. Moreover, Pyun[25] found that H^+ and Cl^- ions could generate a synergic effect. Therefore, under the combined of Cl^- and imposed AC, the instability of passive film becomes much worse, causing a further drop in the anti-corrosion resistance of SDSS.

4. CONCLUSIONS

A rapid increase in i_p and an apparent drop in E_p as well as the significant decrease in R_f and R_{ct} values suggest that the addition of Cl^- and applied AC result in an obviously harmful effect on the passive film, and enhance the dissolution rate of film. The change in N_D and N_A values indicates that the presence of Cl^- or AC application reduces the compactness of film, increases the amount of defects, and weakens the protective ability. Especially at the combined action of Cl^- and imposed AC, the instability of passive film becomes much worse, causing a further decrease in the anti-corrosion resistance of SDSS. AC facilitates the adsorption of Cl^- and H^+ ions on the defects within passive film.

ACKNOWLEDGEMENTS

This work was supported by the Natural Science Foundation of Zhejiang Province (No. LY18E010004) and National Material Environmental Corrosion Infrastructure.

References

1. E.Z. Zhou, H.B. Li, C.T. Yang, J.J. Wang and T.Y. Gu, *Int. Biodeter. Biodegr.*, 127(2018)1.
2. H.Tan, Z.Y.Wang, Y.M.Jiang, D.Han, J.F.Hong, L.D.Chen, L.Z.Jiang and J.Lin, *Corros. Sci.*, 53(2011)2191.
3. L. Bertolini, F. Bolzoni, T. Pastore and P. Pedefferri, *Br. Corros. J.*, 31(1996)218.
4. A. Bautista, G. Blanco, F. Velasco, A. Gutierrez, S. Palacin, L. Soriano and H. Takenouti, *Mater. Construcc.*, 57(2007)17.
5. A. Bautista, G. Blanco, F. Velasco and M.A. Martínez, *Constr. Build. Mater.*, 21(2007)1267.
6. M. C. Alonso, F. J. Luna and M. Criado, *Constr. Build. Mater.*, 199(2019)385.
7. R. D. Moser, P. M. Singh, L. F. Kahn, K. E. Kurtis and Z. B. McClelland, *Constr. Build. Mater.*, 203(2019)366.
8. M. Chen, H. B. Liu, L. B. Wang, C. X. Wang and V. Ji, *Surf. Coat. Tech.*, 344(2018)132.
9. Z. Y. Zhang, H. Z. Zhang, J. Hu, X. X. Qi and Y. Q. Zhao, *Constr. Build. Mater.*, 168(2018)338.
10. N.W. Dai, J. Wu, L.C. Zhang, Y.T. Sun, Y.Y. Liu, Y.Y. Yang, Y.M. Jiang and J. Li, *Mater. Corros.*, 70(2019)419.
11. D.K. Kim, S.V. Muralidharan, T.H. Ha, J.H. Bae, Y.C. Ha, H.G. Lee and J.D. Scantlebury, *Electrochim. Acta*, 51(2006)5259.
12. M. Liu, X. Cheng, X. Li, Z. Jin and H. Liu, *Constr. Build. Mater.*, 93(2015)884.
13. E. C. Paredes, A. Bautista, S. M. Alvarez and F. Velasco, *Corros. Sci.*, 58(2012)52.
14. M. Zhu, C.W. Du, X.G. Li, Z.Y. Liu, H. Li and D.W. Zhang, *Corros. Sci.*, 87(2014)224.
15. M. Zhu, C.W. Du, X.G. Li, Z.Y. Liu, S.R. Wang, J.K. Li and D.W.Zhang, *Electrochim. Acta*, 117(2014)351.
16. R. G. Duarte, A. S. Castela, R. Neves, L. Freire and M. F. Montemor, *Electrochim. Acta*, 124(2014) 218.
17. M. Zhu and C.W. Du, *J. Mater. Eng. Perform.*, 26(2017)221.
18. V.A. Alves and C.M.A. Brett, *Electrochim. Acta*, 47(2002)2081.
19. J.Q. Kang, Y.F. Yang, X. Jiang and H.X. Shao, *Corros. Sci.*, 50(2008)3576.
20. Z. Li, C. Zhang and L. Liu, *J. Alloy. Comp.*, 650(2015)127.
21. H.R. Wang, C.W. Du, Z.Y. Liu, L.T. Wang and D. Ding, *Materials*, 10(2017)851.
22. J. Amri, T. Souier, B. Malki and B. Baroux, *Corros. Sci.*, 50(2008)431.
23. M. Hasegawa and M. Osawa, *Corrosion*, 39(1983)115.
24. R. Ruetschi and R. Giovanoli, *J. Electrochem. Soc.*, 145(2001)2663.
25. S. Pyun, C. Lim and R.A. Oriani, *Corros. Sci.*, 33(1992)437.

© 2020 The Authors. Published by ESG (www.electrochemsci.org). This article is an open access article distributed under the terms and conditions of the Creative Commons Attribution license (<http://creativecommons.org/licenses/by/4.0/>).